

L-3-*n*-Butylphthalide Improves Cognitive Impairment and Reduces Amyloid- β in a Transgenic Model of Alzheimer's Disease

Ying Peng,^{1,2} Jing Sun,¹ Stephanie Hon,¹ Alyssa N. Nylander,¹ Weiming Xia,¹ Yipu Feng,² Xiaoliang Wang,² and Cynthia A. Lemere¹

¹Center for Neurologic Diseases, Brigham and Women's Hospital, Harvard Medical School, Boston, Massachusetts 02115, and ²Institute of Materia Medica, Chinese Academy of Medical Sciences and Peking Union Medical College, Beijing 100050, China

Alzheimer's disease (AD) is an age-related, progressive neurodegenerative disorder that occurs gradually and results in memory, behavior, and personality changes. L-3-*n*-butylphthalide (L-NBP), an extract from seeds of *Apium graveolens* Linn (Chinese celery), has been demonstrated to have neuroprotective effects on ischemic, vascular dementia, and amyloid- β (A β)-infused animal models. In the current study, we examined the effects of L-NBP on learning and memory in a triple-transgenic AD mouse model (3xTg-AD) that develops both plaques and tangles with aging, as well as cognitive deficits. Ten-month-old 3xTg-AD mice were given 15 mg/kg L-NBP by oral gavage for 18 weeks. L-NBP treatment significantly improved learning deficits, as well as long-term spatial memory, compared with vehicle control treatment. L-NBP treatment significantly reduced total cerebral A β plaque deposition and lowered A β levels in brain homogenates but had no effect on fibrillar A β plaques, suggesting preferential removal of diffuse A β deposits. Furthermore, we found that L-NBP markedly enhanced soluble amyloid precursor protein secretion (α APPs), α -secretase, and PKC α expression but had no effect on steady-state full-length APP. Thus, L-NBP may direct APP processing toward a non-amyloidogenic pathway and preclude A β formation in the 3xTg-AD mice. The effect of L-NBP on regulating APP processing was further confirmed in neuroblastoma SK-N-SH cells overexpressing wild-type human APP₆₉₅ (SK-N-SH APPwt). L-NBP treatment in 3xTg-AD mice also reduced glial activation and oxidative stress compared with control treatment. L-NBP shows promising preclinical potential as a multitarget drug for the prevention and/or treatment of Alzheimer's disease.

Introduction

Alzheimer's disease (AD) is the most common form of senile dementia, characterized by progressive memory loss. Neuropathological hallmarks of AD include extracellular senile plaques and intracellular neurofibrillary tangles (Selkoe, 1994). Amyloid- β protein (A β), the core of senile plaque, is a 39–43 amino acid peptide; A β oligomers and aggregates are considered to play a central role in the onset and progression of AD (Chen et al., 2000; Walsh et al., 2002). A β is derived by proteolysis of an integral membrane protein known as the amyloid precursor protein (APP) (Kang et al., 1987). APP is a single-pass transmembrane protein and can be cleaved in at least two pathways: amyloidogenic and non-amyloidogenic. The amyloidogenic pathway involves β - and γ -secretase, cleaving APP at the N and C termini of A β , respectively, and releasing A β into the extracellular space (Haass et al., 1992; Shoji et al., 1992). The alternative pathway involves activa-

tion of α -secretase, now believed to be a member of the disintegrin and metalloprotease (ADAM) families (Lammich et al., 1999; Slack et al., 2001). This processing cleaves APP within the sequence of A β peptide, releasing a soluble APP fragment (α APPs) into the extracellular media, thereby precluding the formation of A β (Esch et al., 1990; Sisodia et al., 1990). The α APPs fragment has been shown to have both neurotrophic (Wallace et al., 1997) and neuroprotective (Mattson et al., 1993; Smith-Swintosky et al., 1994; Gralle et al., 2009) activities. Recent studies suggest that α APPs might serve as an AD therapeutic target (Etcheberrigaray et al., 2004; Small et al., 2005; Turner et al., 2007).

L-3-*n*-Butylphthalide (L-NBP) was extracted as a pure component from seeds of *Apium graveolens* Linn, Chinese celery. Afterward, DL-3-*n*-butylphthalide was synthesized and approved by the State Food and Drug Administration of China for clinical use in stroke patients in 2002. NBP is a chiral compound and contains L and D isomers that have been recently isolated and synthesized. Previous studies showed that L-NBP significantly improved microcirculation in pial arterioles (Xu and Feng, 1999), reduced the area of cerebral infarct and inhibited platelet aggregation (Peng et al., 2004, 2005), improved mitochondrial function and decreased oxidative damage (Dong and Feng, 2002), reduced neuronal apoptosis (Chang and Wang, 2003), and inhibited increases in intracellular calcium levels and the inflammatory re-

Received Jan. 20, 2010; revised April 8, 2010; accepted April 30, 2010.

This work was supported by Alzheimer's Association Grant IIRG-06-27532 (C.A.L.). We thank Dr. Guiquan Chen for help with experiments and Dr. Frank M. Laferla for providing 3xTg-AD mouse breeders. We also thank Dr. Peter Davies for the generous gift of the antibodies used in these studies.

Correspondence should be addressed to Dr. C. A. Lemere, Center for Neurologic Diseases, Harvard New Research Building, Room 636F, 77 Avenue Louis Pasteur, Boston, MA 02115. E-mail: clemere@rics.bwh.harvard.edu.

DOI:10.1523/JNEUROSCI.0340-10.2010

Copyright © 2010 the authors 0270-6474/10/308180-10\$15.00/0

Table 1. Primary antibodies used in this study

Antibody	Immunogen	Host	Dilution	Application	Source
R1736	Residues 595–611 of APP695 (α APPs)	Rabbit	1:1000	WB	D. Selkoe (Center for Neurologic Diseases, Boston, MA)
R1282	A β _{1–40}	Rabbit	1:1000	IHC	D. Selkoe
C8	Against last 20 C-terminal residues of APP	Rabbit	1:1000	WB	D. Selkoe
IDE-1	Residues 62–73 of human IDE-1	Rabbit	1:1000	WB	D. Selkoe
PKC α	C terminus of PKC α of human origin	Mouse	1:1000	WB	Santa Cruz Biotechnology
ADAM10	Residues 732–748 of human ADAM10	Rabbit	1:200	WB	Sigma
TACE	C terminal of human TACE	Rabbit	1:200	WB	ProSci
CD45	Mouse B-cells	Rat	1:5000	IHC	Serotec
GFAP	Bovine GFAP	Rabbit	1:1000	IHC	Dako
AT8	Phospho-Ser202/Thr205	Mouse	1:25	IF	Pierce
AT180	Phospho-Thr231/Ser235	Mouse	1:50	IF	Pierce
PHF-1	Phospho-Ser396/Ser404	Mouse	1:100	IF	P. Davies (Albert Einstein College of Medicine, Bronx, NY)

IHC, Immunohistochemistry; IF, immunofluorescent staining; WB, Western blot.

sponse (Xu and Feng, 2000) in experimental ischemic animal models. Recently, we found that L-NBP alleviated the learning and memory deficits induced by chronic cerebral hypoperfusion in rats (Peng et al., 2007b). In A β intracerebroventricularly infused rats, oral gavage with L-NBP significantly improved cognitive impairment and inhibited oxidative injury, neuronal apoptosis, and glial activation (Peng et al., 2009). Furthermore, in primary neurons and neuroblastoma SH-SY5Y cells, L-NBP attenuated A β -induced neuronal apoptosis (Peng et al., 2008). These results suggest that L-NBP might have potential as an AD therapeutic.

In this study, we examined the effect of L-NBP on cognitive impairment in a triple-transgenic mouse model of AD (3xTg-AD mice). Moreover, we investigated the mechanisms underlying the efficacy of the compound (e.g., APP processing, A β generation and clearance, and glial activation).

Materials and Methods

Animals and treatment. L-NBP (purity >98%) was synthesized by the Department of Medical Synthetic Chemistry, Institute of Materia Medica and dissolved in vegetable oil at a concentration of 15 mg/ml. In this study, 3xTg-AD mice expressing mutant human genes APP^{swe}, PS1^{M146V}, and tau^{P301L} generated by Dr. Frank M. LaFerla (University of California at Irvine, Irvine, CA) were used (Oddo et al., 2003a). The mice were originally generated in a hybrid 129/C57BL/6 genetic background but were backcrossed for multiple generations onto a C57BL/6 single background. In this model, intracellular A β is apparent between 3 and 6 months of age, and A β deposition is evident by 12 months of age. Long-term potentiation is severely impaired in 6-month-old mice (Oddo et al., 2003b). In addition, the 3xTg-AD mice have been shown to exhibit cognition impairment by 6 months of age (Billings et al., 2005). Therefore, we treated 3xTg-AD mice for 18 weeks, starting at 10 months of age, assuming these mice had already developed cognitive impairment, as published previously. However, since our study was conducted, a genetic drift has been observed in this line of mice outside of the LaFerla laboratory (Hirata-Fukae et al., 2008). At the time of our study, the 3xTg-AD mice in our colony developed plaque deposition between 10 and 12 months, but we did not run a pretest to determine whether they were already cognitively impaired before the onset of L-NBP treatment.

The 3xTg-AD mice were divided into two groups: one received L-NBP treatment and the other received vegetable oil alone (vehicle control group). L-NBP was administered by oral gavage 5 d/week at a dose of 15 mg/kg body weight ($n = 8$, four males and four females). A control group ($n = 9$, five males and four females) received oral gavage in the same manner using vegetable oil without L-NBP. The body weight of each mouse was recorded every 2 weeks. After behavioral testing was completed, the mice were killed by CO₂ inhalation, and blood was collected by cardiac puncture, followed by transcardial perfusion with 20–30 ml PBS. The brain was removed. One hemisphere was snap frozen in liquid nitrogen and stored at -80°C until analysis, and the other hemisphere was

fixed in 4% paraformaldehyde for 2 h, followed by incubation in graded sucrose at 4°C. All animal use was approved by the Harvard Standing Committee for Animal Use and was in compliance with all state and federal regulations.

Morris water maze. The Morris water maze task was used to evaluate the drug-related changes in learning and memory in mice (Morris, 1984). Briefly, the apparatus consisted of a circular metal pool (160 cm in diameter) filled with water made opaque by the addition of white beads. A translucent acrylic platform (10 cm in diameter), located in the center of the northwest or southeast quadrant, was placed 1.5 cm under the surface of the water. There were prominent visible cues around the room. The mouse was gently released with its nose against the wall into the water from one of the four preplanned starting positions (north, south, east, or west). The swimming path of each mouse was tracked using Watermaze 2020 software (HVS Image).

Spatial learning training. Spatial training of the hidden platform in the water maze was performed for 5 consecutive days. On each day, training consisted of three blocks, with each interblock interval being 2 h. In each block, there were two consecutive training trials, and the intertrial interval was 15 s. The starting position for each trial was pseudorandomly chosen and counterbalanced across all the experimental groups. The mice were given a maximum of 60 s to find the hidden platform. If a mouse failed to find the platform within 60 s, the training was terminated, a maximum score of 60 s was assigned, and the mouse was manually guided to the hidden platform. The mouse was allowed to stay on the platform for 30 s before it was removed from the pool.

Probe trial. Two probe trials were performed, one at 2 h and another at 48 h after the last training trial (day 5), to assess short-term and long-term memory consolidation, respectively. The platform was removed and the mice were placed into the pool from the quadrant opposite to the training quadrant. Starting positions were counterbalanced across mice. In each probe trial, the mice were allowed to swim for 60 s.

Immunohistochemistry and histology. Ten micrometer sagittal cryosections of mouse brain were mounted on glass slides. The primary antibodies used in the study are summarized in Table 1. Secondary biotinylated antibodies (anti-mouse, anti-rat, and anti-rabbit) and secondary antibodies for immunofluorescent staining were obtained from Vector Laboratories and Invitrogen. Immunohistochemical staining was performed as described previously, with the hippocampus as region of interest (ROI) (Maier et al., 2008). Thioflavin S (Thio S) staining for fibrillar A β was performed by incubating slides in a 1% aqueous solution of Thioflavin S for 10 min, followed by rinsing in 80 and 95% ethanol and then distilled water. For immunofluorescent staining with AT8, AT180, and PHF-1, sections were first pretreated with 0.01 M Tris-buffered saline (TBS) and then blocked with 2% goat serum in TBS for 5 min. The sections were incubated with the primary antibodies overnight at 4°C, followed by secondary antibodies (1:200 in TBS plus 2% goat serum) for 2 h at room temperature. To quantify immunoreactivity and Thioflavin S staining, acquisition of images was performed in a single session using a QICAM camera (Q-imaging) mounted on an Olympus BX50 microscope. Image analysis was performed using IP Lab Spectrum 3.1 Image

Analyzer software. The threshold of detection was held constant during analysis. For all treatment groups, the percentage area occupied by A β , Thio S, and glial immunoreactivity in the hippocampal area, including CA regions, dentate gyrus, and dorsal subiculum, was calculated for three equidistant sections per mouse, whereas phosphorylated tau immunoreactivity in the same hippocampal regions was calculated for four equidistant sections per mouse.

Western blot. The brains were homogenized in 5 vol of TBS with a protease inhibitor cocktail (Roche Applied Science) and phosphatase inhibitors (50 mM sodium fluoride, 2 mM sodium orthovanadate, and 10 mM sodium pyrophosphate). The samples were centrifuged at $175,000 \times g$ for 30 min. The pellets were resuspended in the same volume of TBS-T (TBS/1% Triton X-100 plus protease inhibitor cocktail and phosphatase inhibitor) buffer, sonicated for 5 min in 4°C water bath, homogenized, and centrifuged at $175,000 \times g$ for 30 min at 4°C. The supernatant of the TBS-T-soluble homogenate was collected and stored at -20°C . The pellets were extracted a third time as described previously (Johnson-Wood et al., 1997) using ice-cold guanidine buffer (5 M guanidine-HCl/50 mM Tris, pH 8.0). These TBS-insoluble fractions were run on 10–20% Tricine gels (Invitrogen), transferred onto 0.2 μm nitrocellulose membranes at 400 mA for 2 h, and then blocked with 5% fat-free milk in 20 mmol/L Tris-HCl, pH 7.4, containing 150 mmol/L NaCl and 0.05% Tween-20 for 2 h at room temperature. Then, the blots were probed with primary antibodies overnight at 4°C, followed by incubation with enhanced chemiluminescence (ECL) anti-rabbit or anti-mouse IgG horseradish peroxidase-linked species-specific whole antibody for 2 h at room temperature. The signal was detected using an ECL kit, scanned, and analyzed by densitometric evaluation using an imaging system and analyzing software (FluorChemTMIS-8800 software; Alpha Innotech). Membranes were reprobed with an antibody against β -actin as a control for protein loading.

Antioxidative assay. Malondialdehyde (MDA), the most abundant lipid peroxide, is widely used to measure lipid peroxidation as an indicator of oxidative stress. MDA levels of brain homogenates were examined by using a BIOOXYTECH MDA-586 kit (Oxis Research) according to the instructions of the manufacturer. In addition, we measured the activities of total antioxidant enzymes and catalase using a BIOXYTECHAOP-450 kit and a BIOXYTECHCatalase-520 kit (Oxis Research), respectively.

Cell culture. Human neuroblastoma SK-N-SH cells overexpressing wild-type APP695 (SK-N-SH APPwt) were a gift from Dr. Dennis Selkoe (Center for Neurologic Diseases, Boston, MA). SK-N-SH APPwt were grown in DMEM containing 10% fetal bovine serum, 100 $\mu\text{g}/\text{ml}$ penicillin, 100 $\mu\text{g}/\text{ml}$ streptomycin, and 200 $\mu\text{g}/\text{ml}$ G418. Cell cultures were incubated at 37°C in a humid 5% CO₂/95% air environment. Cells were grown until nearly confluent, washed with serum-free medium, and incubated in serum-free medium for 18–24 h. For detection of α APPs, full-length APP, A β , ADAMs, protein kinase C α (PKC α), and cell viability, the cells were incubated with L-NBP for 24 h. In addition, in the other determinations, cells were preincubated with ADAMs and PKC inhibitors for 30 min and then coincubated with L-NBP plus inhibitor for 24 h. After incubation with the drugs or control treatments for the indicated periods, conditioned media were collected and mixed with a complete protease inhibitor cocktail (Roche Applied Science). The media were centrifuged at $3000 \times g$ for 10 min to remove cellular debris. Supernatants were concentrated with Amicon Ultra-4 centrifugal filter devices (Millipore Corporation). The concentrated conditioned medium was stored at -20°C . Cells were washed twice with ice-cold PBS and lysed with 500 μl of 1% NP-40 in 50 mmol/L Tris HCl, pH 7.6, 150 mmol/L NaCl, 2 mmol/L EDTA, and complete protease inhibitor mixture as described previously (Peng et al., 2007a). Aliquots of lysates were spun at 14,000 rpm for 10 min, and the supernatants were stored at -20°C . To ensure equal loading, protein levels were determined using the DC Protein Assay (Bio-Rad).

Cell viability. Cell viability was evaluated using a Cell Viability kit (Promega) according to the instructions of the manufacturer. Cells were cultured in 96-well plates. After treatment with L-NBP or control treatment for 24 h, 15 μl of dye solution was added to each well. The plate was incubated at 37°C for 4 h in a humidified, 5% CO₂ atmosphere. Then,

100 μl of the solubilization solution was added to each well, and the plates were allowed to stand overnight at room temperature to completely solubilize the formazan crystals. The absorbance was recorded at a 570 nm wavelength using a 96-well plate reader.

ELISA for A β levels. A β levels were measured in the conditioned medium of SK-N-SH APPwt cells and brain homogenates (TBS-, TBS-T-, and guanidine-soluble fractions) using specific A β _{3–40}, A β _{3–42}, and A β _{1–total} ELISAs as reported previously (Peng et al., 2006).

Statistical analysis. Prism software (GraphPad Software) was used to analyze the data. All data were expressed as mean \pm SEM. A value of $p < 0.05$ was considered statistically significant. Treatment differences in the escape latency in the water maze task were analyzed using repeated-measures ANOVA. The chance performance of probe trial in the water maze was analyzed by one-sample t test. In addition, treatment differences in the probe trials and biochemical and pathological assays were analyzed using the Mann–Whitney U test. The *in vitro* studies were analyzed using a one-way ANOVA, followed by a Newman–Keuls *post hoc* test. Each of the *in vitro* experiments was repeated three to six times.

Results

Oral L-NBP treatment ameliorated the spatial learning and some memory deficits in 3xTg-AD mice

We carefully monitored the general health of 3xTg-AD mice during L-NBP treatment and did not find any abnormal changes. In addition, the body weights of mice were not significantly different between L-NBP-treated and vehicle control mice (data not shown). Together, these data indicate that L-NBP had no significant toxicity in mice.

After L-NBP treatment, at the age of 15 months, the 3xTg-AD mice were tested behaviorally. Morris water maze test, one of the most widely accepted behavioral tests of hippocampal-dependent spatial learning and memory (Morris, 1984), was used to monitor the spatial learning and memory in the mice. Spatial learning was assessed by the time required to find the hidden platform (escape latency). Figure 1A shows the results of all mice during water maze acquisition training. Repeated-measures ANOVA revealed a significant day effect on escape latency ($F_{(4,60)} = 14.76$; $p < 0.001$) within the groups, suggesting that all L-NBP-treated mice improved their spatial learning effectively across the 5 d training period. In addition, we found a significant treatment effect ($F_{(1,15)} = 5.72$; $p < 0.05$) on the escape latency demonstrating that L-NBP was effective in attenuating spatial learning deficits in 3xTg-AD mice.

Furthermore, we investigated the effects of L-NBP on spatial memory deficits in 3xTg-AD mice. Probe trials were conducted to assess the short-term memory at 2 h and long-term memory at 48 h after training on day 5 and day 7, respectively (Fig. 1C). Vehicle control mice did not spend significantly more time searching for the platform in the target quadrant (where the platform had been located previously) relative to chance performance (25%). However, L-NBP-treated mice spent significantly more time searching in the target quadrant relative to chance performance in both the 2 h short-term and 48 h long-term memory tests ($45.3 \pm 9.49\%$, $p < 0.05$ and $57.15\% \pm 7.81\%$, $p < 0.001$, respectively; one-sample two-tailed t test). Even so, in the short-term probe trial, the difference in performance between vehicle and L-NBP-treated mice was not significant. In contrast, in the long-term spatial reference memory test, L-NBP-treated mice spent significantly more time in the target quadrant compared with the vehicle control mice ($p < 0.05$). Treatment groups were gender matched and showed no significant gender differences.

To exclude the possibility that the improvement of L-NBP on spatial learning and memory in 3xTg-AD mice was not attribut-

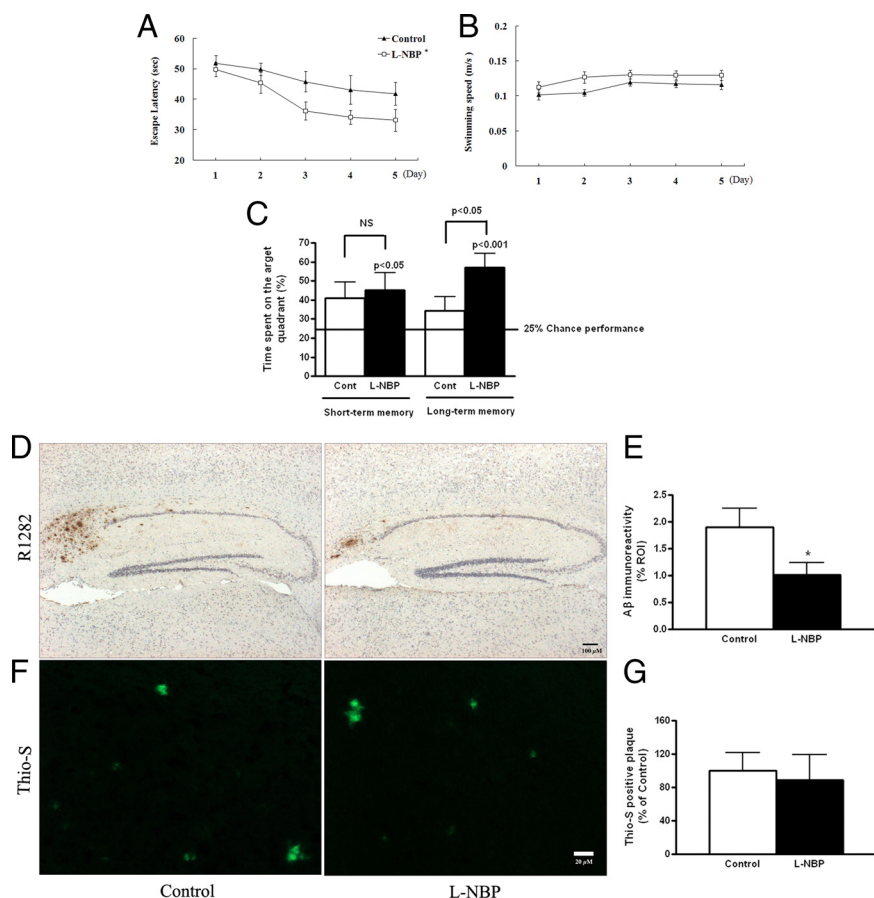


Figure 1. Long-term L-NBP treatment improved spatial learning and memory deficits and reduced total A β plaque burden in 3xTg-AD mice. **A**, Acquisition of spatial learning was assessed in the Morris water maze hidden platform task. Latency score represents the time taken to escape to the platform once the mouse is put in the water. All mice showed significant improvement in escape latency with successive days of training, indicating that the learning deficits in the 3xTg-AD mice were significantly attenuated by L-NBP treatment compared with vehicle control mice. **B**, No significant differences were observed in motor function of the L-NBP-treated mice and the vehicle controls as reflected by the swimming speed. **C**, L-NBP improved short-term (day 5) and long-term (48 h; day 7) memory in the probe trial. L-NBP treatment significantly increased the time spent searching for the hidden platform in the target quadrant compared with 25% chance performance whether in day 5 and day 7. Furthermore, compared with the control-treated mouse, L-NBP-treated mice spent significantly more time searching for the hidden platform in the target quadrant on day 7 ($p < 0.05$). There was no significant difference between L-NBP-treated and control-treated 3xTg-AD mice in short-term spatial memory. **D**, Total plaque load (including diffuse and compacted fibrillar plaques), using the A β antibody R1282, was significantly decreased in the hippocampus of L-NBP-treated 3xTg-AD mice compared with vehicle controls. **F**, Fibrillar, compact plaques labeled by Thioflavin S were not significantly different between treatment groups. **E**, **G**, Quantitative image analysis was performed for R1282 immunoreactivity (**E**) and Thioflavin S (**G**). Values represent group mean \pm SEM. Eight to nine mice were tested per group. * $p < 0.05$ versus vehicle control group. The horizontal line marks chance performance.

able to sensorimotor abnormalities, we first analyzed swimming ability. As shown in Figure 1B, there was no difference on swimming speed between the two groups of mice across the 5 training days. Moreover, we analyzed thigmotaxis, a measure of anxiety level in the water maze, and did not find any evidence of elevated thigmotaxic behavior in either group during the 5 d training period (data not shown).

To further exclude the possibility that 3xTg-AD mice may have developed abnormal basic learning or vision acuity problem, we used a visible cued task to test the same mice in the water maze. The 3xTg-AD mice did not exhibit any impairment in the cue task performance (data not shown). Thus, these results confirmed that the 3xTg-AD mice display normal basic spatial learning or vision acuity.

L-NBP reduced cerebral plaque deposition and A β levels in 3xTg-AD mice

To determine whether the improvement of L-NBP on the learning and memory deficits correlated with changes in A β levels in the brain, all mice were killed after behavioral testing. The brains were removed for biochemical and immunohistochemical analyses. Total A β plaque load, including diffuse and compacted, fibrillar plaques, was detected by A β immunolabeling with a general A β polyclonal antibody, R1282 (a gift from Dr. D. Selkoe) (Fig. 1D), and fibrillar amyloid deposits by Thioflavin S staining (Fig. 1F). Long-term oral administration of L-NBP significantly reduced total A β plaque burden in the hippocampus, particularly in the dorsal subiculum ($p < 0.05$) (Fig. 1E). However, L-NBP had no effect on Thio S-positive plaque deposition, indicating that L-NBP preferentially reduced nonfibrillar, diffuse A β plaques (Fig. 1G). Next, we analyzed cerebral A β levels by ELISA. L-NBP treatment partially lowered A β levels in TBS-soluble, TBS-T-soluble, and guanidine-soluble brain homogenates (Fig. 2A–I). In particular, significant reductions were observed in TBS-T-soluble A β_{1-42} ($p < 0.05$) and guanidine-soluble A β_{1-42} ($p < 0.01$) levels in L-NBP-treated mouse brain compared with vehicle controls. In addition, L-NBP had a tendency to lower TBS-soluble A β_{x-42} levels ($p = 0.07$). These data confirm that L-NBP had some A β -lowering effect *in vivo*.

L-NBP attenuated glial activation in 3xTg-AD mice

Activated astrocytes and microglia are associated with A β plaque deposition in the brains of AD patients and transgenic AD mouse models (Itagaki et al., 1989; Matsuoka et al., 2001). In our previous study, L-NBP was shown to attenuate astrocyte activation in A β intracerebroventricularly infused rats (Peng et al., 2009). Thus, we investigated the ability of L-NBP treatment to suppress astrocyte and microglial reactivity in the current study. Serial sections were stained with an anti-A β antibody (R1282), an anti-GFAP antibody for astrocytes, and an anti-CD45 antibody for microglia (Fig. 3A). Immunostaining of GFAP showed that reactive astrocytes were abundant and closely associated with A β deposits in 3xTg-AD mice. L-NBP treatment significantly reduced GFAP immunoreactivity by 31% compared with vehicle control mice ($p < 0.05$) (Fig. 3B). CD45-immunoreactive activated microglia were evident in and around A β plaque deposits in 3xTg-AD mice. Overall, activated microglia were reduced by ~30% in the L-NBP-treated mice relative to the vehicle control mice, but the difference was not significant (Fig. 3C), possibly because of the high variability observed between animals within groups.

L-NBP directed APP processing toward the non-amyloidogenic pathway in 3xTg-AD mice

Our data demonstrated that L-NBP treatment attenuated cognitive impairment and lowered A β plaque deposition and A β levels in the brain. To identify the underlying mechanism, we investigated the effect of L-NBP on APP processing, α APPs, and full-length APP by Western blot measurement. We chose the polyclonal antibody R1736 (a gift from Dr. D. Selkoe), which was raised in rabbits against residues 595–611 of APP695 and labels α APPs as a 98 kDa band and full-length APP at ~110 kDa. L-NBP treatment significantly stimulated the release of α APPs ($p < 0.05$) (Fig. 4A, B), suggesting that L-NBP may mediate APP processing toward the non-amyloidogenic pathway. It has been reported that increased APP synthesis may lead to elevated APP secretion. Therefore, we next determined the effect of L-NBP on full-length APP levels by using the C-terminal APP polyclonal antibody C8 (a gift from Dr. D. Selkoe). L-NBP treatment had no effect on APP steady-state levels, further suggesting that L-NBP affected APP processing but not APP synthesis (Fig. 4A, B).

ADAM family enzymes catalyze the shedding of the ectodomain of APPs and other membrane proteins (Allinson et al., 2003). ADAM 10 and ADAM17 were examined in the current study because of their relevance to Alzheimer's disease (Buxbaum et al., 1998; Lammich et al., 1999). L-NBP treatment significantly increased ADAM10 and ADAM17 levels (Fig. 4A). Quantitative analysis showed a 50% elevation in ADAM10 levels ($p < 0.01$) and a 70% increase in ADAM17 levels ($p < 0.05$) after L-NBP treatment (Fig. 4C). These data provide additional evidence that L-NBP may mediate APP processing via the α -secretase pathway.

Reduced A β levels may also reflect A β degradation. Insulin degrading enzyme (IDE) is one of the main proteolytic enzymes responsible for cerebral A β degradation (Farris et al., 2003). Using a specific IDE polyclonal antibody (a gift from Dr. D. Selkoe) for Western blotting, we found that L-NBP-treated mice showed a nonsignificant trend for increased IDE expression in the brain compared with vehicle control mice ($p = 0.08$) (Fig. 4A, C). Thus, it might be possible that L-NBP lowering of A β burden may be attributable, in part, to modest acceleration of A β degradation, although additional studies in a larger number of mice are needed to confirm this very preliminary finding.

A number of reports indicate that PKC is involved in the regulation of APP processing (Nitsch et al., 1992; Peng et al., 2007a). PKC agonist phorbol esters have been shown to increase α APPs release and decrease A β levels (Checler, 1995; Chen and Fernandez, 2004). In particular, PKC α has been demonstrated to be involved in non-amyloidogenic cleavage of APP (Kinouchi et al., 1995). PKC α was assessed by Western blot. As shown in Figure 4, A and B, a significant 33% increase in PKC α expression was observed in L-NBP-treated mice compared with vehicle control mice ($p < 0.05$), indicating that L-NBP might enhance PKC α

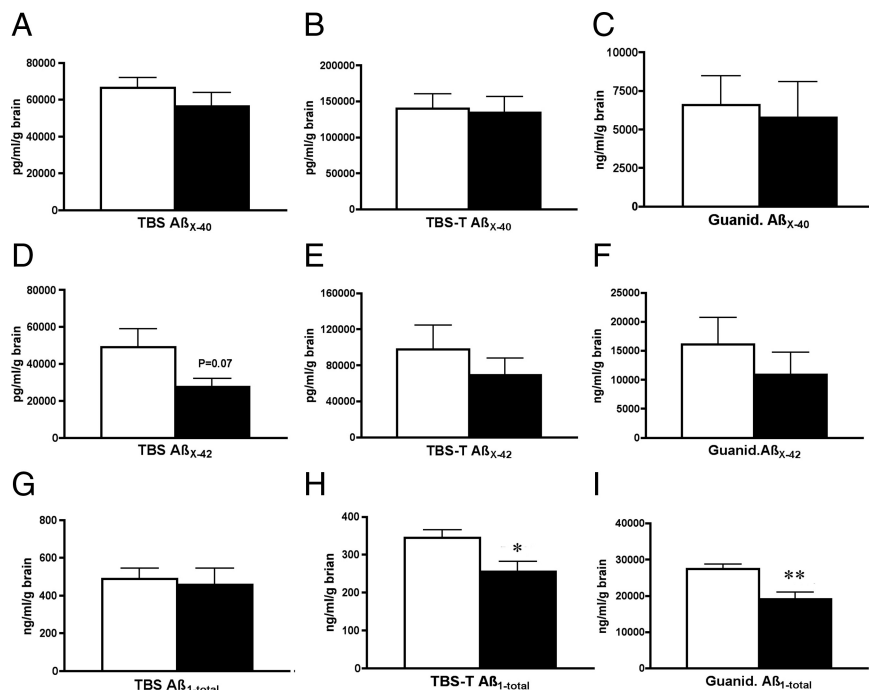


Figure 2. L-NBP treatment demonstrated some A β -lowering effects in brain homogenates of L-NBP-treated mice (black bars) compared with vehicle control-treated mice (white bars) using A β -specific ELISAs (A–I). A–C, A β_{x-40} levels were not changed after L-NBP treatment. D–F, A β_{x-42} levels of brain homogenates showed a trend ($p < 0.07$) for lower A β_{x-42} levels in TBS-soluble extracts of brain homogenates in L-NBP-treated 3xTg-AD mice (D). G–I, Compared with vehicle control 3xTg-AD mice, L-NBP treatment markedly decreased TBS-T-soluble A $\beta_{1-total}$ extracts ($p < 0.05$) and TBS-insoluble guanidine A $\beta_{1-total}$ extracts of brain homogenates ($p < 0.01$). Values represent group mean \pm SEM. $n = 8–9$ mice per group. * $p < 0.05$, ** $p < 0.01$ versus vehicle control group.

signaling, thereby directing APP processing toward to non-amyloidogenic pathway.

L-NBP decreased oxidative stress in 3xTg-AD mice

In the 3xTg AD mouse model, it had been demonstrated that oxidative stress occurs at an early stage, before the appearance of A β plaques and neurofibrillary tangles (Resende et al., 2008). MDA, a lipid peroxidation end product, is an indicator of oxidative stress (Jackson, 1999). In this study, the MDA levels of the brain were examined by spectrophotometric assay. MDA levels were significantly reduced in L-NBP-treated mice compared with vehicle control mice ($p < 0.05$), suggesting that L-NBP may prevent oxidative stress injury. Modest and nonsignificant increases in total antioxidants and catalase were observed in L-NBP-treated 3xTg-AD mice compared with control-treated mice (data not shown).

L-NBP modestly lowered AT8 phosphorylated tau immunoreactivity but overall had no significant effect on tau protein phosphorylation

Hyperphosphorylated tau appears in the 3xTg-AD mouse brain after the onset of A β deposition (Oddo et al., 2003b). In an A β intracerebroventricularly infused rat model, we found that L-NBP reduced tau abnormal hyperphosphorylation by inhibiting glycogen synthase kinase-3 β activity (Peng et al., 2009). Given the beneficial effects of L-NBP on lowering A β deposition and regulating APP processing, we explored a possible role of L-NBP in tau protein hyperphosphorylation in 3xTg-AD mice. Tau hyperphosphorylation was determined by immunofluorescent staining using specific antibodies against different phosphorylation sites on tau, including monoclonal antibodies: AT8

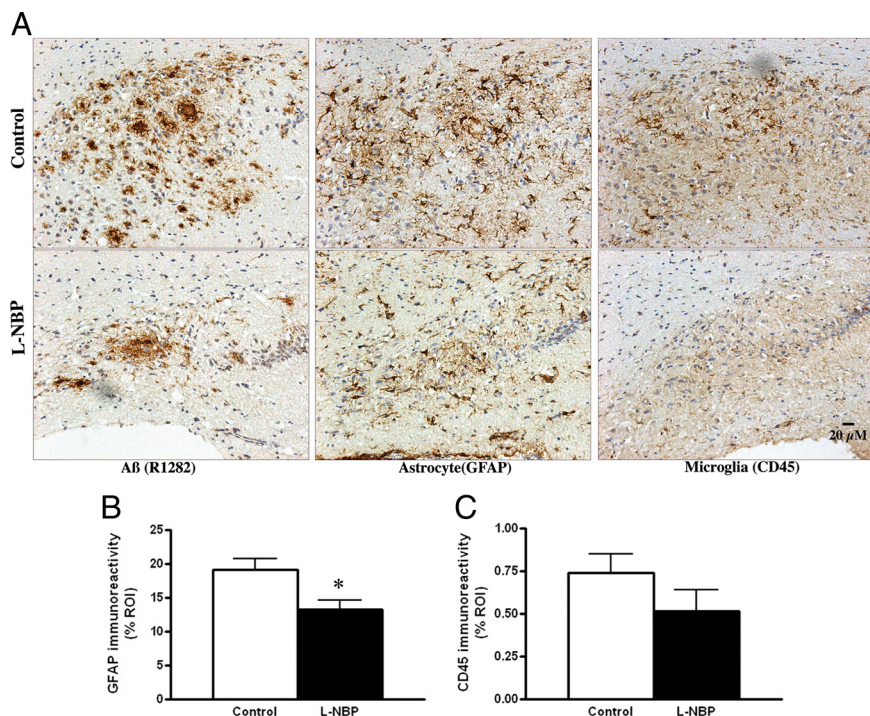


Figure 3. L-NBP treatment reduced glial activation in the hippocampus of 3xTg-AD mice. **A**, Immunohistochemical analysis of hippocampus of representative serial sections of a vehicle control-treated animal (top) and an L-NBP-treated animal (bottom). L-NBP reduced the total plaque load. In parallel, the number of GFAP-positive astrocytes and CD45-positive microglia were also decreased after chronic L-NBP treatment. **B**, Quantitative image analysis of GFAP immunoreactivity demonstrated that reactive astrocytes were significantly decreased in L-NBP-treated mice ($p < 0.05$). **C**, CD45 immunoreactivity was modestly and nonsignificantly attenuated in L-NBP-treated mice compared with vehicle control-treated mice. Values represent group mean \pm SEM. $n = 8$ –9 mice per group. * $p < 0.05$ versus vehicle control group.

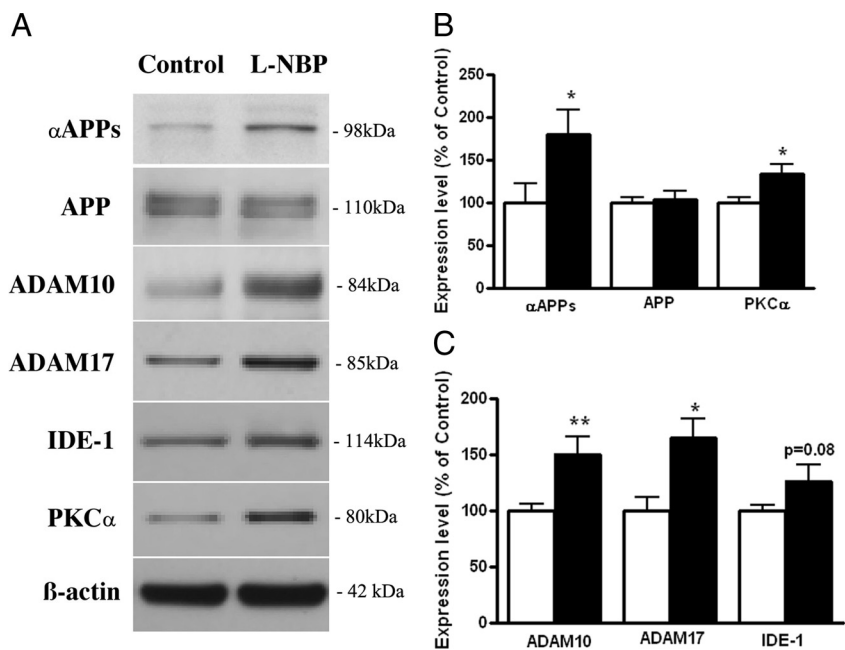


Figure 4. L-NBP treatment promoted α APPs release and elevated ADAM10, ADAM17, and PKC α levels in 3xTg-AD mice. **A**, Representative Western blots of α APPs, APP, ADAM10, ADAM17, IDE-1, and PKC α in the brain homogenates of 3xTg-AD mice treated with vehicle control and L-NBP, respectively, are shown. **B**, **C**, Quantitative analysis of α APPs, APP, and PKC α (**B**) and ADAM10, ADAM17, and IDE-1 (**C**). Quantified results were normalized to β -actin expression. Values were expressed as percentages compared with vehicle control mice (set to 100%) and represented as group mean \pm SEM. $n = 8$ –9 mice per group. * $p < 0.05$, ** $p < 0.01$ versus vehicle control group.

(recognizing the Ser202 and Thr205 residues), AT180 (recognizing the Thr231 residue), and PHF-1 (recognizing the Ser396 or Ser404 residues; gift from Dr. P. Davies, Albert Einstein College of Medicine, Bronx, NY). AT8, AT180, and PHF-1 immunoreactivities were found in scattered neurons and neuronal processes of the CA1 and dorsal subiculum in the vehicle control 3xTg-AD mice (supplemental Fig. 1A, available at www.jneurosci.org as supplemental material). L-NBP treatment nonsignificantly decreased AT8 immunoreactivity by 35.5% compared with vehicle control treatment ($p = 0.35$) (supplemental Fig. 1B, available at www.jneurosci.org as supplemental material). AT180 and PHF-1 immunoreactivities were similar between L-NBP- and vehicle control mice (supplemental Fig. 1C,D, available at www.jneurosci.org as supplemental material) and, therefore, unaffected by L-NBP treatment.

L-NBP increased α APPs release and diminished A β generation in APP-transfected SK-N-SH cells

To validate our *in vivo* studies, we performed *in vitro* studies to determine whether L-NBP treatment could promote non-amyloidogenic APP processing and α -secretase proteolysis and impact A β levels in neuroblastoma SK-N-SH APPwt cells. First, we examined the effect of L-NBP on regulating the release of α APPs into the conditioned media in SK-N-SH APPwt cells. Western blot with antibody R1736 revealed that, after a 24 h treatment of the cells with L-NBP, α APPs secretion was elevated in a concentration-dependent manner. At the dose of 0.1 μ M, L-NBP increased α APPs release by 75% ($p < 0.05$). The maximal effect of L-NBP was observed at a concentration of 10 μ M, which resulted in a twofold increase in α APPs levels compared with the control ($p < 0.001$) (Fig. 5A,B). These data suggest that L-NBP mediated APP processing toward the non-amyloidogenic pathway. Next, we evaluated the effect of L-NBP on cellular APP levels after 24 h of treatment. Whole-cell lysates were analyzed by Western blot by using an APP antibody, C8. L-NBP treatment had no effect on APP steady-state levels, further suggesting that L-NBP affected APP processing but not APP synthesis (Fig. 5A,C).

ELISA results showed that A β_{x-40} , A β_{x-42} , and A $\beta_{1-total}$ production were dose dependently reduced after 24 h of treatment with L-NBP. Particularly at the high concentration of 10 μ M L-NBP, A β_{x-40} , A β_{x-42} , and A $\beta_{1-total}$ levels were significantly reduced by

25% ($p < 0.01$), 34% ($p < 0.05$), and 31% ($p < 0.05$), respectively (Fig. 5D–F). Cell viability was examined after 24 h of incubation with L-NBP at 0–10 μM , but L-NBP had no effect on cell viability (Fig. 5G). Cell proliferation and growth rates were unchanged by L-NBP treatment (data not shown). Thus, it appears that L-NBP was nontoxic to SK-N-SH APPwt cells, and the reduction in A β levels was not attributable to cell death.

Next, we chose C-terminal polyclonal antibodies to detect ADAM10 and ADAM17 expression at the cellular membrane. After 24 h incubation, L-NBP partially increased the ADAM10 and ADAM17 levels in a dose-dependent manner. However, the difference between L-NBP-treated cells and control cells did not reach significance (supplemental Fig. 2A–D, available at www.jneurosci.org as supplemental material). We speculated that L-NBP might regulate the activities of ADAMs at an earlier stage. To address this issue, the cells were preincubated with the ADAM17 inhibitor tumor necrosis factor- α protease inhibitor-2 (TAPI-2) at 10 μM and the ADAM10 inhibitor matrix metalloproteinase-9 (MMP-9)/MMP-13 at 2 μM for 30 min and then coincubated with the inhibitors and 10 μM L-NBP for 24 h. The results are shown in Figure 5, H and I. L-NBP markedly enhanced αAPPs release ($p < 0.01$). The ADAM10 and ADAM17 inhibitors blocked the L-NBP-mediated αAPPs elevation ($p < 0.05$), further confirming that the effect of L-NBP on APP processing is regulated via α -secretase and that ADAM10 and ADAM17 are likely involved.

To determine whether PKC signaling is involved in the L-NBP-induced increase in αAPPs release, we directly detected PKC α expression in the SK-N-SH APPwt cells. Incubation of L-NBP for 24 h dose dependently elevated PKC α levels, especially at the 10 μM dose at which the increase was significant ($p < 0.05$) (Fig. 5J,K). A PKC signaling-specific inhibitor, GF109203X (2-[1-(3-dimethylaminopropyl)-1H-indol-3-yl]-3-(1H-indol-3-yl)maleimide) (2.5 μM), was used to preincubate the cells for 30 min before and throughout L-NBP treatment. αAPPs release induced by L-NBP was significantly reduced by the PKC inhibitor, indicating that the PKC signaling pathway may be involved in L-NBP-induced αAPPs release ($p < 0.001$) (Fig. 5L,M).

Discussion

L-NBP may be a promising candidate for the treatment of AD because it has been shown to alleviate the cognitive impairment induced by A β intracerebroventricular infusion in rats *in vivo* (Peng et al., 2009) and reduce A β -induced neuronal apoptosis *in vitro* (Peng et al., 2008). Until now, the actual therapeutic value of L-NBP on AD pathology and cognitive deficits has not been dem-

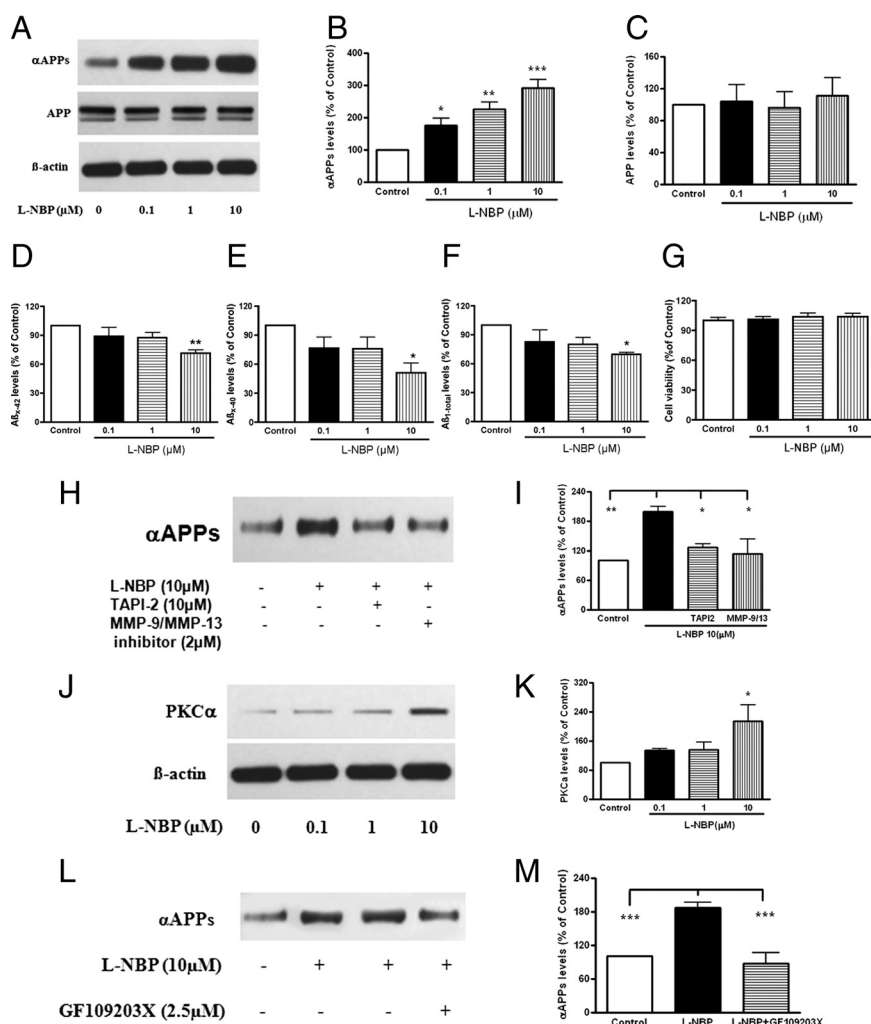


Figure 5. L-NBP increased the αAPPs release, reduced A β generation, and had no effect on full-length APP level and cell viability in cultured neuroblastoma SK-N-SH APPwt cells. α -Secretase and PKC α may be involved in L-NBP-regulated APP processing toward the non-amyloidogenic pathway. Cells were incubated with L-NBP at each of three concentrations (0.1, 1, or 10 μM) or without L-NBP (control) for 24 h. **A**, Media were collected, and αAPPs and steady-state levels of APP were detected with polyclonal antibodies R1736 and C8, respectively, using Western blot. **B**, **C**, Quantitative analysis of the Western blot was expressed as a percentage of αAPPs (**B**) and APP (**C**) from control cells. **D–F**, A β_{x-42} , A β_{x-40} , and A $\beta_{1\text{-total}}$ levels of the medium were detected by specific ELISAs. L-NBP dose dependently reduced A β levels. **G**, Cell viability was evaluated using a Cell Viability kit (MTT analysis). Cell viability of neuroblastoma cells was unchanged after L-NBP incubation. **H**, **I**, Cells were preincubated for 30 min with vehicle alone or with 10 μM TAPI-2 or 2 μM MMP-9/MMP-13 and then co-incubated with the inhibitor with or without L-NBP for an additional 24 h. The inhibitors of TACE/ADAM17 and ADAM10 partially inhibited L-NBP-induced αAPPs secretion. **J**, **K**, L-NBP increased PKC α levels dose dependently. **L**, **M**, A specific inhibitor of PKC (GF109203X) reduced L-NBP-induced αAPPs release in neuroblastoma SK-N-SH APPwt cells. Cells were preincubated with the PKC inhibitor for 30 min and then with the inhibitor with or without L-NBP for an additional 24 h. αAPPs in the media was detected by polyclonal APP antibody, R1736, using Western blot. Results are shown as the mean \pm SEM and represent six independent experiments. * $p < 0.05$, ** $p < 0.01$, *** $p < 0.001$ versus control group or L-NBP group.

onstrated. Our study demonstrates for the first time that L-NBP treatment by oral gavage reduced A β plaque deposition, gliosis, and oxidative stress and improved spatial learning and long-term memory deficits in 3xTg-AD mice.

A number of studies have shown that A β plaque deposition occurs before or early in stages of neurodegeneration and behavioral changes in AD patients (Selkoe, 2001). Recently, soluble A β was demonstrated to induce spatial memory deficits in AD animal models (Billings et al., 2005; Lesné et al., 2006). Our results showed that L-NBP significantly improved spatial learning and long-term spatial memory deficits in 3xTg-AD mice. In the short-term memory probe trial (2 h after the last training session),

L-NBP-treated mice performed better than chance but not significantly better than vehicle control mice. The same mice showed significantly better learning on the same day (day 5) compared with the vehicle controls. The discrepancy in these results could be attributable to treatment differences in learning versus memory (although there was a significant treatment effect in long-term memory on day 7) and more variability in the 2 h probe trial and/or the small number of mice in each group.

L-NBP treatment decreased aggregated TBS-T-soluble and guanidine-soluble A $\beta_{1\text{-total}}$ levels in brain homogenates as well as R1282-immunoreactive A β plaque deposition but not Thio S fibrillar plaques in the brains of 3xTg-AD mice. The A β pellets in the TBST-soluble and guanidine-soluble fractions include diffuse and aggregated, fibrillar plaque material. However, Thio S staining detects mainly β -pleated sheet, fibrillar amyloid plaques, whereas R1282 detects both diffuse and fibrillar A β deposits. Thus, we believe that L-NBP reduced diffuse A β plaques preferentially over fibrillar, compacted A β plaques that were relatively sparse to begin with in our mice. L-NBP showed a nonsignificant but strong trend for reducing soluble A β levels and, therefore, may also have an effect on potentially neurotoxic soluble A β oligomers. L-NBP reduced A $\beta_{1\text{-total}}$ but did not change A β_{x-40} /A β_{x-42} levels. The discrepancy suggests the possibility that L-NBP may have an effect on the N-terminal cleavage of A β by β -secretase (BACE). A previous study demonstrated that BACE1 prefers the A β_1 site, whereas BACE2 prefers internal cleavage sites within A β_{1-40} , such as the A β_{19} or A β_{20} sites and the A β_{34} site (Shi et al., 2003). Investigation of the effects of L-NBP on BACE cleavage of APP is underway in long-term L-NBP prevention and treatment studies in 3xTg-AD mice in our laboratory.

A recent report (Hirata-Fukae et al., 2008) described a slowing of the progression of pathology in the 3xTg-AD model compared with the initial reports. We, too, have made the same observation. At the time we initiated our study, the 10- to 11-month-old mice in our colony had only very low amounts of plaque deposition, most of which was limited to the subiculum. We did not perform water maze testing on 10- to 11-month-old mice at that time, so we are unable to confirm whether the mice were already cognitively impaired as suggested by previous publications. Thus, it is possible that the beneficial effects of L-NBP on cognitive impairment and A β deposition may have been attributable to prevention or delaying of the pathological and cognitive changes rather than reversing preexisting pathology and/or cognitive deficits.

It appears that the effect by L-NBP of lowering cerebral A β accumulation may be attributable to directing APP processing toward a non-amyloidogenic pathway. Our study confirmed that L-NBP enhanced α APPs release and precluded A β generation. α APPs has been shown to be beneficial for memory function and possesses neuroprotective and neurotrophic properties (Mattson, 1997). It is possible that α APPs derived from L-NBP-mediated APP processing may serve as a neuroprotective agent and contribute to the long-term benefit of L-NBP on memory in 3xTg-AD mice.

Members of the ADAM family have been put forward as candidate α -secretases (Buxbaum et al., 1998). ADAM10 and tumor necrosis factor- α converting enzyme (TACE)/ADAM17 are considered likely candidates for α -secretase APP cleavage (Lammich et al., 1999; Nunan and Small, 2000). Our study shows that L-NBP long-term treatment promoted non-amyloidogenic APP processing *in vitro* and *in vivo*, by promoting α -secretase cleavage of APP. In our 3xTg-AD mice study, ADAM10 and TACE protein levels were significantly elevated in L-NBP-treated mice. In SK-N-SH APPwt cells, L-NBP led to a trend for increased ADAM10

and TACE protein levels. We speculated that the effect of L-NBP on ADAM10 and TACE might occur at an early stage and gradually disappear. To understand the effects of ADAM10 and TACE clearly, we chose the selective, competitive inhibitors MMP-9/MMP-13 and TAPI-2 to determine the role of ADAM10 and TACE on L-NBP-regulated α APPs release and found that the effects of L-NBP were partially inhibited. Together, these results indicate that ADAM10 and TACE may be involved in L-NBP-induced APP processing.

PKC messenger pathways have been shown to be involved in regulating the non-amyloidogenic processing of APP (Buxbaum et al., 1993; Hung et al., 1993), although not through APP phosphorylation (Hung and Selkoe, 1994). Instead, PKC seems to change α -secretase activities or APP trafficking by protein phosphorylation (Koo, 1997; Skovronsky et al., 2000). In our study, the role of PKC α in the L-NBP-mediated increase in α APPs release was demonstrated *in vivo* and *in vitro*. The long-term treatment of L-NBP significantly upregulated PKC α levels in the brains of 3xTg-AD mice. This effect was confirmed by treatment of SK-N-SH APP cells with L-NBP. In addition, the PKC-specific inhibitor GF109203X partially inhibited L-NBP-induced α APPs release, suggesting that the PKC pathway may be involved in L-NBP-regulated α APPs release.

A β reduction could also occur via increased A β clearance mechanisms, such as upregulating expression of A β cleaving enzymes, including IDE and neprilysin. Endogenous IDE is considered a major soluble protease involved in the degradation of A β in the brain. Here, L-NBP partially increased IDE expression in the treated 3xTg-AD mice, but the difference was not significant ($p < 0.08$). Thus, L-NBP may have some potential to promote A β degradation by activating IDE, thereby lowering A β plaque deposition in brain, but a larger study is needed to further assess this possibility.

Oxidative stress is one of the earliest events in the development and progression of AD pathology (Nunomura et al., 2001). In 3xTg-AD mice, vitamin E and glutathione, two non-enzymatic antioxidants, were shown to be decreased and the levels of several lipid peroxidation markers were increased before the appearance of A β plaques and neurofibrillary tangles (Resende et al., 2008). In the current study, we found that L-NBP significantly reduced the level of lipid peroxidation. In addition, L-NBP modestly and nonsignificantly increased the activities of the total antioxidant enzymes and catalase (data not shown). Our data suggest that the antioxidant effects of L-NBP may be beneficial and act synergistically with other mechanisms for the treatment of AD. Inflammation has long been hypothesized to play a critical role in AD (Griffin, 2006). In 3xTg-AD mice, activation of microglia and astrocytes was markedly enhanced and coincided with the appearance of cognitive deficits and synaptic dysfunction in these mice (Oddo et al., 2003b; Billings et al., 2005; Janelsins et al., 2005). Activation of microglia and astrocytes was reduced in L-NBP-treated 3xTg-AD mice. The inhibitory effect of L-NBP on gliosis may be secondary to the lowering of the A β plaque burden. However, L-NBP has been shown to have a direct anti-inflammatory effect independent of A β (Peng et al., 2007b). Additional studies of L-NBP on neuroinflammation are ongoing, but the anti-inflammatory effect of L-NBP demonstrated here provide additional evidence of the therapeutic potential of L-NBP for AD.

Oddo et al. (2003b) reported that AT180- and AT8-immunoreactive neurons were readily apparent between 12 and 15 months of age, and PHF-1 staining became evident by 18 months of age in 3xTg-AD mice. In the present study, the

3xTg-AD mice were 15 months of age at the time of they were killed. We observed only sparse staining of hyperphosphorylated tau, indicating that these mice were still in early stages of tau pathology. At this stage, L-NBP seemed to have minimal (AT8) or no (AT180 and PHF-1) effect on tau protein hyperphosphorylation. It is possible that the study ended too early to see major effects on tau pathology, such as the formation of PHF-1-immunoreactive dystrophic neurites or neurofibrillary tangles. In addition, it is possible that L-NBP might delay rather than prevent tau pathology. A large study is underway to explore the long-term effects of L-NBP on tau pathology in older 3xTg-AD.

In conclusion, our data demonstrate that L-NBP was able to reduce cerebral A β levels, glial activation, oxidative stress, and cognitive impairment in the 3xTg-AD mouse model. In addition, we found that L-NBP regulated APP processing toward the non-amyloidogenic pathway and promoted α APPs release, thereby precluding A β generation. L-NBP appears to be promising as a multitarget drug for the prevention and/or treatment of Alzheimer's disease.

References

- Allinson TM, Parkin ET, Turner AJ, Hooper NM (2003) ADAMs family members as amyloid precursor protein alpha-secretases. *J Neurosci Res* 74:342–352.
- Billings LM, Oddo S, Green KN, McGaugh JL, LaFerla FM (2005) Intranuclear A β causes the onset of early Alzheimer's disease-related cognitive deficits in transgenic mice. *Neuron* 45:675–688.
- Buxbaum JD, Koo EH, Greengard P (1993) Protein phosphorylation inhibits production of Alzheimer amyloid beta/A4 peptide. *Proc Natl Acad Sci U S A* 90:9195–9198.
- Buxbaum JD, Liu KN, Luo Y, Slack JL, Stocking KL, Peschon JJ, Johnson RS, Castner BJ, Cerretti DP, Black RA (1998) Evidence that tumor necrosis factor alpha converting enzyme is involved in regulated alpha-secretase cleavage of the Alzheimer amyloid protein precursor. *J Biol Chem* 273:27765–27767.
- Chang Q, Wang XL (2003) Effects of chiral 3-n-butylphthalide on apoptosis induced by transient focal cerebral ischemia in rats. *Acta Pharmacol Sin* 24:796–804.
- Checler F (1995) Processing of the beta-amyloid precursor protein and its regulation in Alzheimer's disease. *J Neurochem* 65:1431–1444.
- Chen G, Chen KS, Knox J, Inglis J, Bernard A, Martin SJ, Justice A, McConlogue L, Games D, Freedman SB, Morris RG (2000) A learning deficit related to age and beta-amyloid plaques in a mouse model of Alzheimer's disease. *Nature* 408:975–979.
- Chen M, Fernandez HL (2004) Stimulation of beta-amyloid precursor protein alpha-processing by phorbol ester involves calcium and calpain activation. *Biochem Biophys Res Commun* 316:332–340.
- Dong GX, Feng YP (2002) Effects of NBP on ATPase and anti-oxidant enzymes activities and lipid peroxidation in transient focal cerebral ischemic rats. *Zhongguo Yi Xue Ke Xue Yuan Xue Bao* 24:93–97.
- Esch FS, Keim PS, Beattie EC, Blacher RW, Culwell AR, Oltsdorf T, McClure D, Ward PJ (1990) Cleavage of amyloid beta peptide during constitutive processing of its precursor. *Science* 248:1122–1124.
- Etcheberrigaray R, Tan M, Dewachter I, Kuiperi C, Van der Auwera I, Wera S, Qiao L, Bank B, Nelson TJ, Kozikowski AP, Van Leuven F, Alkon DL (2004) Therapeutic effects of PKC activators in Alzheimer's disease transgenic mice. *Proc Natl Acad Sci U S A* 101:11141–11146.
- Farris W, Mansourian S, Chang Y, Lindsley L, Eckman EA, Frosch MP, Eckman CB, Tanzi RE, Selkoe DJ, Guenette S (2003) Insulin-degrading enzyme regulates the levels of insulin, amyloid beta protein, and the β -amyloid precursor protein intracellular domain in vivo. *Proc Natl Acad Sci U S A* 100:4162–4167.
- Gralle M, Botelho MG, Wouters FS (2009) Neuroprotective secreted amyloid precursor protein acts by disrupting amyloid precursor protein dimers. *J Biol Chem* 284:15016–15025.
- Griffin WS (2006) Inflammation and neurodegenerative diseases. *Am J Clin Nutr* 83:470S–474S.
- Haass C, Schlossmacher MG, Hung AY, Vigo-Pelfrey C, Mellon A, Ostaszewski BL, Lieberburg I, Koo EH, Schenk D, Teplow DB (1992) Amyloid beta-peptide is produced by cultured cells during normal metabolism. *Nature* 359:322–325.
- Hirata-Fukae C, Li HF, Hoe HS, Gray AJ, Minami SS, Hamada K, Niikura T, Hua F, Tsukagoshi-Nagai H, Horikoshi-Sakuraba Y, Mughal M, Rebeck GW, LaFerla FM, Mattson MP, Iwata N, Saido TC, Klein WL, Duff KE, Aisen PS, Matsuoka Y (2008) Females exhibit more extensive amyloid, but not tau, pathology in an Alzheimer transgenic model. *Brain Res* 1216:92–103.
- Hung AY, Selkoe DJ (1994) Selective ectodomain phosphorylation and regulated cleavage of beta-amyloid precursor protein. *EMBO J* 13:534–542.
- Hung AY, Haass C, Nitsch RM, Qiu WQ, Citron M, Wurtman RJ, Growdon JH, Selkoe DJ (1993) Activation of protein kinase C inhibits cellular production of the amyloid beta-protein. *J Biol Chem* 268:22959–22962.
- Itagaki S, McGeer PL, Akiyama H, Zhu S, Selkoe D (1989) Relationship of microglia and astrocytes to amyloid deposits of Alzheimer disease. *J Neuroimmunol* 24:173–182.
- Jackson MJ (1999) An overview of methods for assessment of free radical activity in biology. *Proc Nutr Soc* 58:1001–1006.
- Janelins MC, Mastrangelo MA, Oddo S, LaFerla FM, Federoff HJ, Bowers WJ (2005) Early correlation of microglial activation with enhanced tumor necrosis factor-alpha and monocyte chemoattractant protein-1 expression specifically within the entorhinal cortex of triple transgenic Alzheimer's disease mice. *J Neuroinflammation* 2:23.
- Johnson-Wood K, Lee M, Motter R, Hu K, Gordon G, Barbour R, Khan K, Gordon M, Tan H, Games D, Lieberburg I, Schenk D, Seubert P, McConlogue L (1997) Amyloid precursor protein processing and A beta42 deposition in a transgenic mouse model of Alzheimer disease. *Proc Natl Acad Sci U S A* 94:1550–1555.
- Kang J, Lemaire HG, Unterbeck A, Salbaum JM, Masters CL, Grzeschik KH, Multhaup G, Beyreuther K, Müller-Hill B (1987) The precursor of Alzheimer's disease amyloid A4 protein resembles a cell-surface receptor. *Nature* 325:733–736.
- Kinouchi T, Sorimachi H, Maruyama K, Mizuno K, Ohno S, Ishiura S, Suzuki K (1995) Conventional protein kinase C (PKC)-alpha and novel PKC epsilon, but not -delta, increase the secretion of an N-terminal fragment of Alzheimer's disease amyloid precursor protein from PKC cDNA transfected 3Y1 fibroblasts. *FEBS Lett* 364:203–206.
- Koo EH (1997) Phorbol esters affect multiple steps in beta-amyloid precursor protein trafficking and amyloid beta-protein production. *Mol Med* 3:204–211.
- Lammich S, Kojro E, Postina R, Gilbert S, Pfeiffer R, Jasionowski M, Haass C, Fahrenholz F (1999) Constitutive and regulated α -secretase cleavage of Alzheimer's amyloid precursor protein by a disintegrin metalloprotease. *Proc Natl Acad Sci U S A* 96:3922–3927.
- Lesné S, Koh MT, Kotilinek L, Kaye R, Glabe CG, Yang A, Gallagher M, Ashe KH (2006) A specific amyloid-beta protein assembly in the brain impairs memory. *Nature* 440:352–357.
- Maier M, Peng Y, Jiang L, Seabrook TJ, Carroll MC, Lemere CA (2008) Complement C3 deficiency leads to accelerated amyloid beta plaque deposition and neurodegeneration and modulation of the microglia/macrophage phenotype in amyloid precursor protein transgenic mice. *J Neurosci* 28:6333–6341.
- Matsuoka Y, Picciano M, Malester B, LaFrancois J, Zehr C, Daeschner JM, Olschowka JA, Fonseca MI, O'Banion MK, Tenner AJ, Lemere CA, Duff K (2001) Inflammatory responses to amyloidosis in a transgenic mouse model of Alzheimer's disease. *Am J Pathol* 158:1345–1354.
- Mattson MP (1997) Cellular actions of beta-amyloid precursor protein and its soluble and fibrillogenic derivatives. *Physiol Rev* 77:1081–1132.
- Mattson MP, Cheng B, Culwell AR, Esch FS, Lieberburg I, Rydel RE (1993) Evidence for excitoprotective and intraneuronal calcium-regulating roles for secreted forms of the beta-amyloid precursor protein. *Neuron* 10:243–254.
- Morris R (1984) Developments of a water-maze procedure for studying spatial learning in the rat. *J Neurosci Methods* 11:47–60.
- Nitsch RM, Slack BE, Wurtman RJ, Growdon JH (1992) Release of Alzheimer amyloid precursor derivatives stimulated by activation of muscarinic acetylcholine receptors. *Science* 258:304–307.
- Nunan J, Small DH (2000) Regulation of APP cleavage by alpha-, beta- and gamma-secretases. *FEBS Lett* 483:6–10.
- Nunomura A, Perry G, Aliev G, Hirai K, Takeda A, Balraj EK, Jones PK, Ghanbari H, Wataya T, Shimohama S, Chiba S, Atwood CS, Petersen RB, Smith MA (2001) Oxidative damage is the earliest event in Alzheimer disease. *J Neuropathol Exp Neurol* 60:759–767.

- Oddo S, Caccamo A, Kitazawa M, Tseng BP, LaFerla FM (2003a) Amyloid deposition precedes tangle formation in a triple transgenic model of Alzheimer's disease. *Neurobiol Aging* 24:1063–1070.
- Oddo S, Caccamo A, Shepherd JD, Murphy MP, Golde TE, Kaye R, Metherate R, Mattson MP, Akbari Y, LaFerla FM (2003b) Triple-transgenic model of Alzheimer's disease with plaques and tangles: intracellular A β and synaptic dysfunction. *Neuron* 39:409–421.
- Peng Y, Zeng X, Feng Y, Wang X (2004) Antiplatelet and antithrombotic activity of L-3-n-butylphthalide in rats. *J Cardiovasc Pharmacol* 43:876–881.
- Peng Y, Xu SF, Wang L, Feng YP, Wang XL (2005) Effect of L-3-n-butylphthalide on cerebral infarct volume in the transient cerebral ischemia rats. *Chin New Drug J* 14:420–423.
- Peng Y, Jiang L, Lee DY, Schachter SC, Ma Z, Lemere CA (2006) Effects of huperzine A on amyloid precursor protein processing and beta-amyloid generation in human embryonic kidney 293 APP Swedish mutant cells. *J Neurosci Res* 84:903–911.
- Peng Y, Lee DY, Jiang L, Ma Z, Schachter SC, Lemere CA (2007a) Huperzine A regulates amyloid precursor protein processing via protein kinase C and mitogen-activated protein kinase pathways in neuroblastoma SK-N-SH cells over-expressing wild type human amyloid precursor protein 695. *Neuroscience* 150:386–395.
- Peng Y, Xu S, Chen G, Wang L, Feng Y, Wang X (2007b) L-3-n-Butylphthalide improves cognitive impairment induced by chronic cerebral hypoperfusion in rats. *J Pharmacol Exp Ther* 321:902–910.
- Peng Y, Xing C, Lemere CA, Chen G, Wang L, Feng Y, Wang X (2008) L-3-n-butylphthalide ameliorates beta-amyloid-induced neuronal toxicity in cultured neuronal cells. *Neurosci Lett* 434:224–229.
- Peng Y, Xing C, Xu S, Lemere CA, Chen G, Liu B, Wang L, Feng Y, Wang X (2009) L-3-n-butylphthalide improves cognitive impairment induced by intracerebroventricular infusion of amyloid- β peptide in rats. *Eur J Pharmacol* 621:38–45.
- Resende R, Moreira PI, Proença T, Deshpande A, Busciglio J, Pereira C, Oliveira CR (2008) Brain oxidative stress in a triple-transgenic mouse model of Alzheimer disease. *Free Radic Biol Med* 44:2051–2057.
- Selkoe DJ (1994) Normal and abnormal biology of the beta-amyloid precursor protein. *Annu Rev Neurosci* 17:489–517.
- Selkoe DJ (2001) Alzheimer's disease: genes, proteins, and therapy. *Physiol Rev* 81:741–766.
- Shi XP, Tugusheva K, Bruce JE, Lucka A, Wu GX, Chen-Dodson E, Price E, Li Y, Xu M, Huang Q, Sardana MK, Hazuda DJ (2003) Beta-secretase cleavage at amino acid residue 34 in the amyloid beta peptide is dependent upon gamma-secretase activity. *J Biol Chem* 278:21286–21294.
- Shoji M, Golde TE, Ghiso J, Cheung TT, Estus S, Shaffer LM, Cai XD, McKay DM, Tintner R, Frangione B (1992) Production of the Alzheimer amyloid beta protein by normal proteolytic processing. *Science* 258:126–129.
- Sisodia SS, Koo EH, Beyreuther K, Unterbeck A, Price DL (1990) Evidence that beta-amyloid protein in Alzheimer's disease is not derived by normal processing. *Science* 248:492–495.
- Skovronsky DM, Moore DB, Milla ME, Doms RW, Lee VM (2000) Protein kinase C-dependent alpha-secretase competes with beta-secretase for cleavage of amyloid-beta precursor protein in the trans-golgi network. *J Biol Chem* 275:2568–2575.
- Slack BE, Ma LK, Seah CC (2001) Constitutive shedding of the amyloid precursor protein ectodomain is up-regulated by tumor necrosis factor- α converting enzyme. *Biochem J* 357:787–794.
- Small CL, Lyles GA, Breen KC (2005) Lipopolysaccharide stimulates the secretion of the amyloid precursor protein via a protein kinase C-mediated pathway. *Neurobiol Dis* 19:400–406.
- Smith-Swintosky VL, Pettigrew LC, Craddock SD, Culwell AR, Rydel RE, Mattson MP (1994) Secreted forms of beta-amyloid precursor protein protect against ischemic brain injury. *J Neurochem* 63:781–784.
- Turner PR, Bourne K, Garama D, Carne A, Abraham WC, Tate WP (2007) Production, purification and functional validation of human secreted amyloid precursor proteins for use as neuropharmacological reagents. *J Neurosci Methods* 164:68–74.
- Wallace WC, Akar CA, Lyons WE (1997) Amyloid precursor protein potentiates the neurotrophic activity of NGF. *Brain Res Mol Brain Res* 52:201–212.
- Walsh DM, Klyubin I, Fadeeva JV, Cullen WK, Anwyl R, Wolfe MS, Rowan MJ, Selkoe DJ (2002) Naturally secreted oligomers of amyloid beta protein potently inhibit hippocampal long-term potentiation in vivo. *Nature* 416:535–539.
- Xu H, Feng Y (1999) Effects of d-3-n-butylphthalide (NBP) on pial arterioles in focal cerebral ischemia rats. *Acta Pharmacol Sin* 34:172–175.
- Xu HL, Feng YP (2000) Inhibitory effects of chiral 3-n-butylphthalide on inflammation following focal ischemic brain injury in rats. *Acta Pharmacol Sin* 21:433–438.